Modelling the atmospheric dispersion of radiotracers in small-scale, controlled detonations: validation of dispersion models using field test data

Kathleen M Thiessen[1,*] [ORCID], Petr Kuča[2], Jan Helebrant[2], Jiří Hůlka[2], Thomas W Charnock[3],
Sohan L Chouhan[4], Juraj Ďuran[5], Vladimir Fuka[6], Govert de With[7], Francesco Mancini[8], Raúl Periáñez[9],
Bee Kiat Tay[10], Dejan Trifunović[11] and Hartmut Walter[12]

[1] Oak Ridge Center for Risk Analysis, Oak Ridge, TN, United States of America
[2] Section of Emergency Preparedness, National Radiation Protection Institute (SÚRO), Prague, Czech Republic
[3] Centre for Radiation, Chemical and Environmental Hazards, Public Health England, Chilton, Didcot, Oxfordshire, United Kingdom
[4] Environment and Waste Technologies Branch, Canadian Nuclear Laboratories, Chalk River, Ontario, Canada
[5] Department of Safety Analyses, VÚJE Inc., Trnava, Slovakia
[6] Department of Atmospheric Physics, Faculty of Mathematics and Physics, Charles University, Prague, Czech Republic
[7] Radiation and Environment Department, Nuclear Research and Consultancy Group (NRG), Arnhem, The Netherlands
[8] Department of Engineering and Radiation Protection, SOGIN S.p.A., Rome, Italy
[9] Departamento de Fisica Aplicada, ETSIA, Universidad de Sevilla, Seville, Spain
[10] DSO National Laboratories, Singapore
[11] State Office for Radiological and Nuclear Safety, Zagreb, Croatia
[12] Federal Office for Radiation Protection, Munich, Neuherberg, Germany
[*] Author to whom any correspondence should be addressed.

E-mail: kmt@orrisk.com

Abstract

A series of modelling exercises, based on field tests conducted in the Czech Republic, were carried out by the 'Urban' Working Groups as part of the International Atomic Energy Agency's Environmental Modelling for Radiation Safety II, Modelling and Data for Radiological Impact Assessment (MODARIA) I and MODARIA II international data compilation and model validation programmes. In the first two of these programmes, data from a series of field tests involving dispersion of a radiotracer, ^{99m}Tc, from small-scale, controlled detonations were used in a comparison of model predictions with field measurements of deposition. In the third programme, data from a similar field test, involving dispersion of ^{140}La instead of ^{99m}Tc, were used. Use of longer-lived ^{140}La as a radiotracer allowed a greater number of measurements to be made over a greater distance from the dispersion point and in more directions than was possible for the earlier tests involving shorter-lived ^{99m}Tc. The modelling exercises included both intercomparison of model predictions from several participants and comparison of model predictions with the measured data. Several models (HotSpot, LASAIR, ADDAM/CSA-ERM, plus some research models) were used in the comparisons, which demonstrated the challenges of modelling dispersion of radionuclides from detonations and the need for appropriate meteorological measurements.

1. Introduction

Several of the model testing programmes organised by the International Atomic Energy Agency (IAEA) have included Working Groups specifically focused on modelling of radioactive contamination in urban environments (reviewed by Thiessen *et al* 2008, 2011, 2022, IAEA 1994, 2012a, 2012b, 2021, 2022, in preparation). One of the areas of interest to these Working Groups has been modelling the dispersion of radioactive contamination from relatively small-scale detonations, which might be relevant for a 'dirty bomb' situation, for example. The availability of data from a series of field tests carried out in the Czech

Republic (Prouza *et al* 2010) made it possible to carry out several modelling exercises in which predicted deposition, based on dispersion modelling, could be compared with measurements of deposition from actual detonation and dispersion events. These field tests formed the basis of five modelling exercises during the EMRAS II (Environmental Modelling for Radiation Safety; 2009–2011), MODARIA I (Modelling and Data for Radiological Impact Assessment; 2013–2015) and MODARIA II (2016–2019) programmes (IAEA 2021, 2022, in preparation). During EMRAS II and MODARIA I, a total of four detonation and dispersion events were modelled, based on field tests at a site in Kamenná, Czech Republic, using ^{99m}Tc (half-life, 6 h) as a radiotracer. The MODARIA II exercise used a single field test at a site in Boletice, Czech Republic, involving ^{140}La (half-life, 1.7 d). The longer half-life of ^{140}La made it possible to obtain a greater number of measurements over a wider area than was possible with ^{99m}Tc.

For each of the field tests, the radiotracer was spread by the detonation of a small amount of explosive. The configuration of the radiotracer and explosive for the Kamenná tests was intended to cause the initial dispersion to occur in a desired direction; at Boletice, the detonation was not constrained, and dispersion occurred in all directions. The field tests occurred in open areas, with and without simulated small buildings in anticipated downwind directions. Both test areas were selected for stable wind conditions under typical meteorological conditions, and key meteorological data were collected before and during the dispersion events. Initial conditions for each of the field tests are summarised in sections 1.1 and 1.2 and full details are available in the reports of the IAEA Working Groups (IAEA 2021, 2022, in preparation).

Measurements obtained for the field tests included dose rates, surface contamination of ground and structures (buildings), activity concentrations in air, particle size distribution, time distribution of dust particles in air and thermo-camera snapshots to record changes in infrared radiation. Video recordings of the detonations were obtained from several vantage points.

Participants in the exercises were asked to predict the surface contamination (Bq m^{-2}) as a function of distance from the detonation site, dose rates (mGy h^{-1}, at 1 m height) as a function of distance from the detonation site and time-integrated activity concentrations in air (Bq m^{-3} min) as a function of height and distance along the centreline of the plume. For each of the five events modelled, the input information provided to participants included the arrangement of detectors and other equipment near the detonation site, time-dependent meteorological data (e.g. wind speed and direction) and the amount of radioactivity involved (tables 1 and 2). Full data (input information plus the resulting measurements of surface contamination, dose rates and time-integrated activity concentrations in air) from two earlier field tests at Kamenná were provided to the participants for use in calibration of models, if desired. Based on one of these earlier field tests, suggested values for particle size distributions, aerosol diameters and deposition velocities were made available to participants. Estimates of column (cloud) dimensions were made from video recordings of each event.

The exercises were carried out as blind tests: only the input information was provided to participants, and comparisons of predictions with measurements were made only after the modelling results had been submitted. Although several endpoints were modelled, the analysis of the results focused primarily on predictions of surface contamination (deposition) (IAEA 2021, 2022, in preparation), and this paper is limited to discussion of predicted surface contamination.

In addition to the modelling exercises described in this paper, data sets from these field tests can also be used for validation of location factors, data assimilation to improve initial modelling results and estimation of a source term based on measurements. For example, Urso *et al* (2014) used surface activity from one of the Kamenná field tests with the HotSpot 2.07.1 model to predict the source term.

1.1. Kamenná tests (IAEA 2021, 2022)

The first sets of field tests were carried out in 2007–2010 by the Czech National Radiation Protection Institute (SÚRO) at a test area belonging to the National Institute for Nuclear, Chemical and Biological Protection in Kamenná, near Prague (figure 1). The detonations were performed in an open field (flat terrain), with and without simulated small buildings. A combined booby-trap explosive system was selected, with the dispersion directed in a pre-selected direction. A set of four steel plates (bottom, back wall, two side walls) surrounded by sandbags was used to direct the release in the expected wind direction at an angle of about 30° to the horizontal (Prouza *et al* 2010). Each test used either 1 or 2 GBq of ^{99m}Tc (as NaTcO$_4$ in 0.9% NaCl liquid solution); ^{99m}Tc has an easily detected gamma energy and a short radioactive half-life (6 h). Filters to collect deposition were distributed over a surface area of approximately 50 m × 40 m in the anticipated direction of the dispersion. Deposition occurred during the first few minutes after the dispersion (Prouza *et al* 2010). Summary information for the four Kamenná tests considered in the EMRAS II and MODARIA I programmes is provided in table 1; the meteorological conditions for the tests are summarised in table 2.

Figure 1. Satellite image of the Kamenná test area, Czech Republic. The grid coordinates and dispersion point are indicated. The grid centreline is rotated approximately 68° to the east. The meteorological station was located at grid coordinates $(0, -5)$ for the test on 5 May 2009, $(8.5, 0)$ for the test on 14 July 2009 and $(0, -20)$ for the tests on 4 May 2010 and 22 June 2010. (Map source: Ortofoto © Czech Office for Surveying, Mapping and Cadastre.)
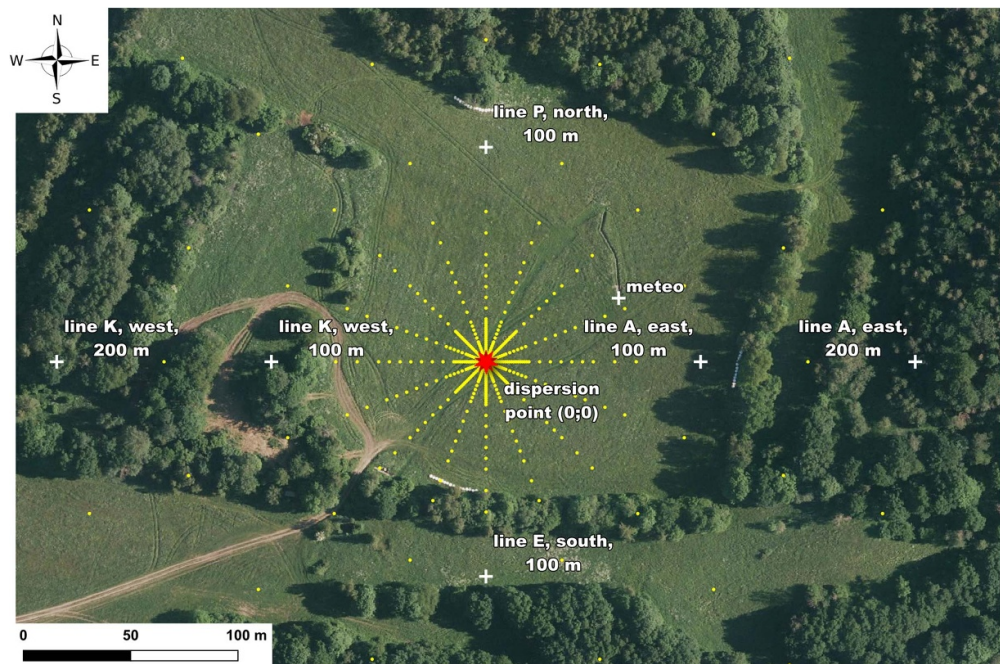
Figure 2. Satellite image of the Boletice test area, Czech Republic. The grid axes and dispersion point are indicated. The meteorological station ('meteo') was located 110 m to the northeast of the dispersion point. (Map source: Ortofoto © Czech Office for Surveying, Mapping and Cadastre.)

1.2. Boletice test (IAEA in preparation)

A later field test was carried out in 2014 in the Boletice military training area in the southern part of the Czech Republic (figure 2). The test used ^{140}La (as LaHNO$_3$ in a 0.1 M HNO$_3$ liquid solution); the total activity was 0.713 GBq. The longer half-life of ^{140}La (1.7 d), together with the larger test area at Boletice,

3

Table 1. Summary information for the field tests used in the exercises.

Programme	Date	Explosion time[a]	Radionuclide and activity (MBq)	Amount of liquid containing the activity	Amount and type of explosive used
Kamenná tests:					
EMRAS II	5 May 2009	12:22	^{99m}Tc, 1222	6 ml	Permon 10T, 350 g
EMRAS II	14 July 2009	12:42	^{99m}Tc, 1088	6 ml	Permon 10T, 350 g
MODARIA I	4 May 2010	14:15	^{99m}Tc, 2119	6 ml	Permon 10T, 350 g
MODARIA I	22 June 2010	12:06	^{99m}Tc, 2045	6 ml	Permon 10T, 350 g
Boletice test:					
MODARIA II	17 June 2014	17:32	^{140}La, 713	4×10 ml	SEMTEX 1A, 250 g

[a] Twenty-four hour system (12:00 = noon).

Table 2. Summary of weather conditions during the field tests[a].

	EMRAS II 5 May 2009	EMRAS II 14 July 2009	MODARIA I 4 May 2010	MODARIA I 22 June 2010	MODARIA II 17 June 2014
Location	Kamenná	Kamenná	Kamenná	Kamenná	Boletice
Temperature (°C)	10.1–10.7	25.4–25.6	10.1–10.2	18.5–18.9	2 m height 13.4–15.4 (mean 13.8); 10 m height 13.2–15.0 (mean 13.5)
Relative air humidity (%)	48–54	56–61	77–79	41–46	2 m height 52–67 (mean 62)
Condensation point (°C)	0.3–1.3	16.1–17.4	6.3–6.7	5.2–6.8	—
Wind speed (m s^{-1})	0.9–2.2	0–0.4	0.9–3.6	1.3–3.1	10 m height 0.02–4.47 (mean 0.78)
Gust wind speed (m s^{-1})	1.3–4.5	0–0.9	2.2–5.8	1.8–4.9	—
Wind direction (degree)	248–293	135–315	90–270	0–270	10 m height 0–359 (mean 241)
Air pressure (hPa)	1021.3–1021.5	1012.6–1012.8	1013.6–1013.7	1013–1013.4	2 m height 929.5–930.2 (mean 929.8)

[a] More detailed meteorological data were provided in electronic form. Measurements were taken at a height of 2 m for the 2009 tests, 10 m for the 2010 tests and at 2 m or 10 m for the 2014 test. The indicated wind direction is the direction the wind was blowing from.

allowed an omnidirectional dispersion event. Filters to collect deposition were distributed in all directions from the detonation point, over an area of about 60 m × 60 m. Summary information for the Boletice test considered in the MODARIA II programme is provided in table 1, and the meteorological conditions for the test are summarised in table 2.

2. Models used in the exercises

Table 3 provides a summary of the models used by participants in these five exercises. Participants volunteered to be involved in the programmes, and most used institutional or off-the-shelf models for these exercises. The models represented three main types of computational approaches to modelling atmospheric dispersion (Gaussian, Lagrangian and computational fluid dynamics (CFD)) and were developed for a variety of purposes, including research, emergency response and decision support (table 3).

Eight models in total were used during the three programmes (EMRAS II, MODARIA I and II). Over the course of these programmes, three participants used the HotSpot model, and three versions of that model were used. During the third programme, the LASAIR model was used by two participants. In all, the EMRAS II exercises included eight participants with seven models, the MODARIA I exercises included three participants with three models and the MODARIA II exercise included three participants with two models. In a few cases it was possible to compare results from two participants using the same model, or from one participant using two models. Tables 4–6 provide summaries of the key parameters and approaches used by participants in each exercise or pair of exercises.

For column dimensions, source partitioning within the column and particle size distributions, individual participants chose whether to use suggested values (e.g. based on earlier field tests), default values in their models or information from other sources. Time-dependent meteorological data were provided to participants; individual participants chose whether to use the time-dependent data or average data,

Table 3. Summary of models used in the dispersion exercises.

Model[a]	Participant	Country	Exercises	Purpose of model	Computational type	Domain size
ADDAM/CSA-ERM	S Chouhan	Canada	EMRAS II, MODARIA I	ADDAM, safety assessment for accidents; CSA-ERM, research tool	Gaussian	ADDAM, plume centreline from 100 m; CSA-ERM, 5 m grid
HotSpot 2.07.01	T Charnock	United Kingdom	EMRAS II	Emergency response	Gaussian	Plume centreline only
HotSpot 2.07.01	D Trifunović	Croatia	EMRAS II	Emergency response	Gaussian	Plume centreline only
HotSpot 3.0.3	T Charnock	United Kingdom	MODARIA II	Emergency response	Gaussian	Nested grid 5 × 5 m to 100 m downwind; 10 × 10 m to 200 m; 50 × 50 m to 1000 m; 100 × 100 m to 2000 m
HotSpot 3.1	F Mancini	Italy	MODARIA II	Emergency response	Gaussian	Plume centreline only
URD[b]	B K Tay	Singapore	MODARIA I	Decision support	Gaussian puff	2 km × 2 km at 10 m resolution; 40 m × 60 m at 1 m resolution
RDD_MMC	J Ďuran	Slovakia	EMRAS II	Not provided	Lagrangian	Not provided
University of Seville	R Periañez	Spain	EMRAS II	Research model	Lagrangian	2000 m downwind, 100 m upwind
LASAIR	H Walter	Germany	EMRAS II, MODARIA I, MODARIA II	Decision support, emergency response	Lagrangian	40 km × 40 km or 20 km × 20 km; 5 m grid, increasing to the outside
LASAIR	F Mancini	Italy	MODARIA II	Emergency response	Lagrangian	20 km × 20 km
CFD	G de With	Netherlands	EMRAS II	Commercial software	CFD	1000 m × 100 m × 2000 m
CLMM[c]	V Fuka	Czech Republic	EMRAS II	Research model	Atmospheric CFD	'small' = up to 50 m; 'large' = up to 2000 m (separate calculations)

[a] ADDAM, Atmospheric Dispersion and Dose Analysis Method; CSA-ERM, Canadian Standards Association Emergency Response Model; URD, Urban Release and Dispersion; RDD-MMC, Radiological Dispersal Device-Method Monte Carlo; LASAIR, LAgrange Simulation of the dispersion [Ausbreitung] and Inhalation of Radionuclides; CFD, computational fluid dynamics; CLMM, Charles University Large Eddy Microscale Model.

[b] The URD model, developed by the Technical University of Denmark (DTU), was used as part of the ARGOS decision support system (developed by PDC-ARGOS) which was being tested and evaluated by the participant's organisation at the time of the exercise.

[c] The CLMM model has since been renamed as ELMM (Extended Large Eddy Microscale Model).

5

Table 4. Summary of selected parameters used in the EMRAS II exercises (Kamenná field tests conducted on 5 May 2009 and 14 July 2009).

Model	Calibration	Atmospheric stability class	Wind speed (m s^{-1})	Wind conditions	Dry deposition velocity (m s^{-1})
ADDAM/CSA-ERM	Yes	5 May 2009, class C 14 July 2009, class A	5 May 2009, 2.7 14 July 2009, 0.726	Not provided[a]	1×10^{-1}
HotSpot 2.07.01 (Charnock)	Yes	5 May 2009, class D 14 July 2009, class C	5 May 2009, 1.5 14 July 2009, 0.4	Not provided	Respirable fraction,[b] 1×10^{-4} Non-respirable fraction, 4×10^{-1}
HotSpot 2.07.01 (Trifunović)	Yes	5 May 2009, class D 14 July 2009, class C	5 May 2009, 1.3 14 July 2009, 0.1	Not provided	Respirable fraction, 8×10^{-4}
RDD_MMC	Not provided	5 May 2009, class B 14 July 2009, class A	5 May 2009, 1.30 14 July 2009, 0.20	Not provided	0.2 μm, 5.0×10^{-3} 1.0 μm, 1.5×10^{-4} 8.0 μm, 1.0×10^{-3} 20.0 μm, 8.0×10^{-3}
University of Seville	Yes	Not applicable	Time-dependent measurements	Transient	Not applicable
LASAIR	No	5 May 2009, class D 14 July 2009, class C	Time-dependent: 5 May 2009, 0.9–7.2 14 July 2009, 0–4.9	Transient	<2.5 μm, 1×10^{-3} 2.5–10 μm, 1×10^{-2} 10–50 μm, 5×10^{-2} >50 μm, 2×10^{-1}
CFD	Yes	Not applicable	5 May 2009, 3.0 14 July 2009, 0.3	Steady state	0.2 μm, 5.0×10^{-5} 1.0 μm, 1.5×10^{-4} 8.0 μm, 1.0×10^{-3} 20.0 μm, 8.0×10^{-3}
CLMM	Not provided	Not applicable	5 May 2009, 2.3 14 July 2009, 0.4	Not provided	Not applicable

(Continued.)

6

Table 4. (Continued.)

Model	Source term partitioning	Column dimensions	Surface roughness	Particle size distribution
ADDAM/CSA-ERM	Not provided	Height = 12.9 m Effective release height = 6.45 m	Grass terrain: roughness length 0.4 m	Not provided
HotSpot 2.07.01 (Charnock)	Source partitioned uniformly up to a height of 5 m	Column height constrained to 13 m	'Standard'[c]	Respirable fraction 0.999 Non-respirable fraction 0.001
HotSpot 2.07.01 (Trifunović)	h1, 0.04 (ground level) h2, 0.16 (0.2 × cloud top) h3, 0.25 (0.4 × cloud top) h4, 0.35 (0.6 × cloud top) h5, 0.20 (0.8 × cloud top)	Cloud top = 13 m	Not provided	Respirable fraction 0.99
RDD_MMC	Not provided	Volume 1 (20%), 13 m × 6 m × 2 m Volume 2 (80%), 4 m × 2 m × 3 m	Not provided	$0.2~\mu m$, 20% $1.0~\mu m$, 15% $8.0~\mu m$, 50% $20.0~\mu m$, 15%
University of Seville	Partitioning between liquid and gas particles	(1) 7 m × 7 m, effective height ± 6 m (2) Cloud top = 13 m	Not applicable	Not applicable
LASAIR	Uniformly distributed within initial cloud	Height 13 m, base 5 m	Test ground, 0.1 m Vicinity, 1.0 m Obstacle, 1.5 m	$0–2.5~\mu m$, 40% $2.5–10~\mu m$, 40% $10–50~\mu m$, 10% $\geqslant 50~\mu m$, 10%
CFD	Not provided	12 m × 7 m × 7 m	Aerodynamic roughness length (y_0), 0.03 m	2×10^{-5} m, 10% 8×10^{-6} m, 46.6% 1×10^{-6} m, 15.0% 2×10^{-7} m, 28.4%
CLMM	h1, 0.04 (ground level) h2, 0.16 (0.2 × cloud top) h3, 0.25 (0.4 × cloud top) h4, 0.35 (0.6 × cloud top) h5, 0.20 (0.8 × cloud top)	Cloud top = 13 m	Ground surface, 3 mm	$0.2~\mu m$, 39.6% $1~\mu m$, 11.8% $8~\mu m$, 37.8% $20~\mu m$, 10.8%

[a] The information was not required by the model or was not provided by the participant.

[b] The respirable fraction is the fraction of aerosolised material that is respirable, generally considered as having an activity median aerodynamic diameter (AMAD) of $\leqslant 10~\mu m$; the non-respirable fraction is the fraction of aerosolized material that has an AMAD > 10 μm. In HotSpot, the respirable fraction is assumed to have an AMAD of 1 μm (Homann 2009).

[c] Model options are 'standard' or 'urban'.

Table 5. Summary of selected parameters used in the MODARIA I exercises (Kamenná field tests conducted on 4 May 2010 and 22 June 2010).

Model	Calibration	Atmospheric stability class	Wind speed (m s^{-1})	Wind conditions	Dry deposition velocity (m s^{-1})
ADDAM/CSA-ERM	Yes	4 May 2010, class A 22 June 2010, class A	4 May 2010, 1.44 22 June 2010, 1.46	4–10 min average (all heights and locations)	1×10^{-1}
URD	No	Not applicable	Time-dependent measurements at 10 m height	Transient: time-dependent measurements at 10 m height	Calculated within the model
LASAIR	No	4 May 2010, class D 22 June 2010, class D	Time-dependent: 4 May 2010, 0.5–3.6 22 June 2010, 0.5–3.6	Transient: time-dependent measurements at 10 m height	<2.5 μm, 1×10^{-3} 2.5–10 μm, 1×10^{-2} 10–50 μm, 5×10^{-2} >50 μm, 2×10^{-1}

Model	Source term partitioning	Column dimensions	Surface roughness	Particle size distribution
ADDAM/CSA-ERM	Not provided[a]	Height = 12.9 m Width = 11 m Effective release height = 6.45 m	Grass terrain: roughness length, 0.4 m	Not provided
URD	Uniformly distributed within the cloud	Height = 11 m Five initial puffs of the same size	Grassland: roughness, 0.05 m	<0.39 μm, 40% 0.39–1.3 μm, 12% 1.2–10.2 μm, 38% >10.2 μm, 10%
LASAIR	Uniformly distributed within the initial cloud	Height = 7 m Base = 3 × 3 m	Test ground, 0.1 m Vicinity (trees), 1.0 m Obstacles, actual heights	0–2.5 μm, 40% 2.5–10 μm, 40% 10–50 μm, 10% ≥50 μm, 10%

[a] The information was not required by the model or was not provided by the participant.

8

Table 6. Summary of selected parameters used in the MODARIA II exercise (Boletice field test conducted on 17 June 2014).

Model	Handling of meteorological data	Atmospheric stability class	Wind speed (m s^{-1})	Wind conditions	Dry deposition velocity (m s^{-1})
HotSpot 3.0.3 (Charnock)	Constant windspeed and direction	Class D	Run (1)[a] 4 Run (2) 1.2	(1) Steady-state, 250° (2) Steady-state, 286°	Respirable fraction (20%), 0.003 Non-respirable fraction (80%), 0.1
HotSpot 3.1 (Mancini)	Median value during interval 17:32:00–17:32:59	Class B	1.33	Steady-state, 291°	Respirable fraction (60%), 0.003 Non-respirable fraction (40%), 0.1
LASAIR (Walter)	Mean value during 1 min intervals (17:32–17:52), starting at 17:34	Class D	Time-dependent, 0.5–1.3	Transient, 214°–298°	<2.5 μm, 1 × 10^{-3} 2.5–10 μm, 1 × 10^{-2} 10–50 μm, 5 × 10^{-2} >50 μm, 1.5 × 10^{-1} 0–10 μm, assumed to be respirable
LASAIR (Mancini)	Mean value during 1 min intervals (17:32–17:41), wind direction shifted by 45°	Class B	Time-dependent, 0.58–1.33	Transient, 291°–326° (wind direction shifted by 45°)	<2.5 μm, 1 × 10^{-3} 2.5–10 μm, 1 × 10^{-2} 10–50 μm, 5 × 10^{-2} >50 μm, 1.5 × 10^{-1} 0–10 μm, assumed to be respirable

Model	Source term partitioning	Column dimensions	Surface roughness	Particle size distribution
HotSpot 3.0.3 (Charnock)	HotSpot default height distribution: 20% at 0.8 height 35% at 0.6 height 25% at 0.4 height 16% at 0.2 height 4% at ground level	Height = 17 m (calculated by HotSpot)	0.01 m	20% respirable 80% non-respirable
HotSpot 3.1 (Mancini)	20% at 0.8 cloud top 35% at 0.6 cloud top 25% at 0.4 cloud top 16% at 0.2 cloud top 4% at ground level	Height = 22 m	0.01 m	<1 μm, 60% >1 μm, 40%
LASAIR (Walter)	Homogeneously distributed in the cloud, released within 1 s	Horizontal extension = 12 m Vertical extension = 19 m	Near (~40 × 50 m), 0.01 m Other areas, 1.0 m	<2.5 μm, 50% <10.0 μm, 30% <50.0 μm, 20%
LASAIR (Mancini)	Homogeneously distributed in the cloud, released within 1 s	Horizontal extension = 12 m Vertical extension = 20 m	0.01 m	<2.5 μm, 20% <10.0 μm, 40% <50.0 μm, 20% >50 μm, 20%

[a] The HotSpot 3.0.3 model was run twice by Charnock. The second model run included an adjustment to the timing of the meteorological data to allow for the distance (110 m) between the meteorological station and the dispersion point; all other input parameters and assumptions were the same between the two model runs (section 5.2).

depending in some cases on model capabilities. The models in these exercises did not treat droplet evaporation.

3. Results of the exercises

The primary result analysed in these exercises involved a comparison of measured and predicted deposition (surface contamination, Bq m^{-2}) within the grid area (up to 50 m from the dispersion point). Sections 4–6 summarise the results of the EMRAS II, MODARIA I and MODARIA II exercises, respectively. The meteorological situations during the field tests are described, followed by a summary of the modelling results and relevant discussion. Details of the analysis for each exercise are described in the Working Group reports (IAEA 2021, 2022, in preparation).

Using the set of grid coordinates corresponding to the measurement locations for each field test, the set of measurements and each set of model predictions was interpolated using a multilevel B-spline interpolation method (Lee *et al* 1997) with SAGA GIS[13] software (for the Kamenná tests, grid north was 68° east of true north). This approach facilitated the characterisation of the measured or predicted deposition (both the dispersion pattern and the degree of contamination) in the entire grid area, as opposed to only at the measurement points.

The contour plots in the figures for each exercise use the same coordinate system and colour scale, thereby enabling a visual comparison of the two-dimensional measured or predicted deposition. The maximum measured and predicted depositions (Bq m^{-2}, with the coordinates of the location) are summarised in tables for each of the respective field tests, along with the total measured and predicted activity deposited in the grid area (MBq) for each field test.

4. EMRAS II exercises (Kamenná field tests 5 May 2009 and 14 July 2009)

4.1. Meteorological situation during the field tests
Figures 3 and 4 show the 1 min averaged wind speed and wind direction for the Kamenná field tests that were conducted on 5 May 2009 and 14 July 2009, respectively. For the first of these (5 May 2009), the wind direction after the detonation was relatively stable, although the wind speed varied from about 1 to 3.5 m s^{-1}. Due to the stable wind direction, the plume generally went in a straight line. However, for the later test (14 July 2009), the detonation was followed by periods of no wind and very low wind speed and with considerable variation in wind direction. Therefore, the plume did not go in the anticipated direction toward the measurement equipment.
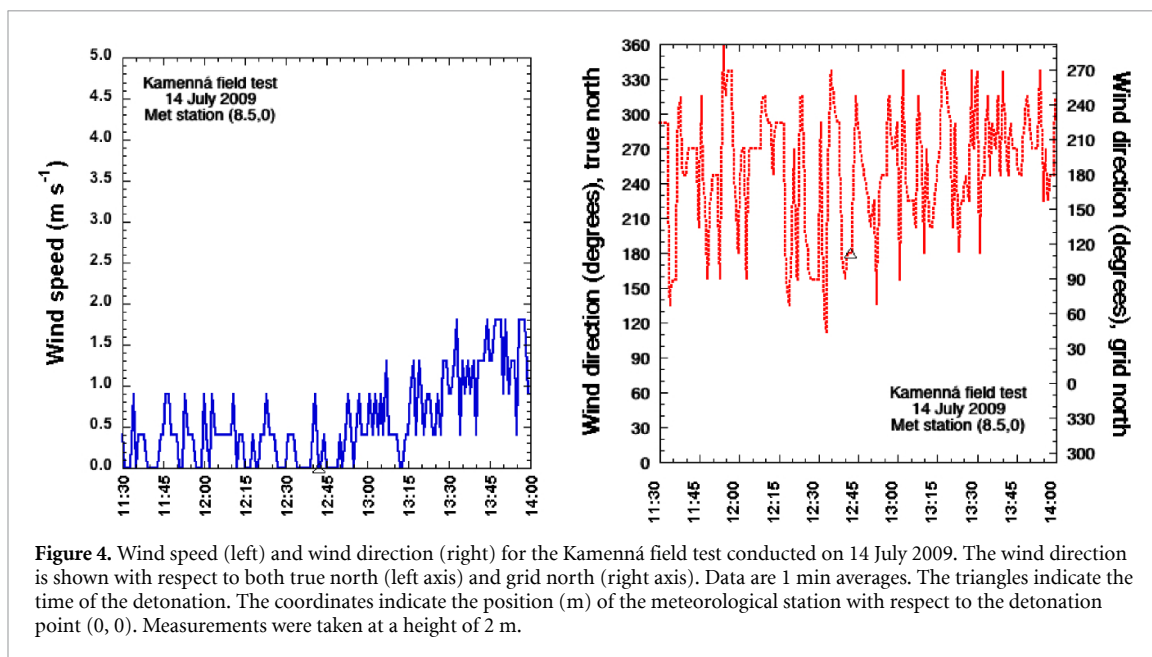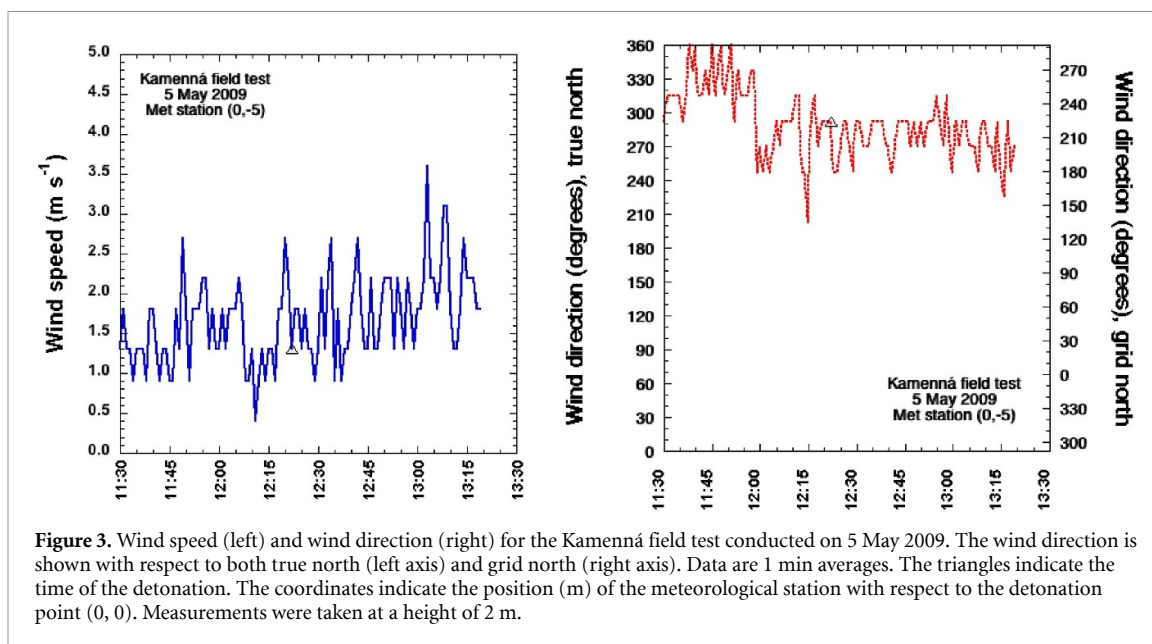
4.2. Results
Figures 5 and 6 provide comparisons of the measured and predicted activity concentrations (deposition, Bq m^{-2}) for the two field tests, respectively. Tables 7 and 8 summarise the maximum measured and predicted deposition (Bq m^{-2}) for each of the field tests, and the total measured and predicted activity deposited in the grid area (MBq) for each field test.

For the first test (5 May 2009), the measurements indicated that deposition occurred primarily to the grid north, while the model predictions ranged from northwest to northeast. The predicted total activity deposited within the grid area ranged from 1.8 to 730 MBq (measured, 36 MBq). The predicted maximum deposition ranged from 1.3×10^3 to 1.0×10^6 Bq m^{-2} (measured, 1.4×10^6 Bq m^{-2}). The plume during this test went almost straight down the *y*-axis of the grid, while most of the predicted plumes were displaced to one side or the other of the *y*-axis (figure 5). The HotSpot 2.07.01 model, with two different users, produced both the lowest and highest predictions for the total activity deposited within the grid area, about a factor of 20 on either side of the measured value. These two modellers used different assumptions for the wind speed, dry deposition velocity and partitioning of the source term. In contrast, predictions from three models (RDD_MMC, University of Seville and LASAIR) were within a factor of 2 of the measured total activity within the grid area, in spite of some differences in the parameterisation of their models.

For the second test (14 July 2009), the measurements indicated deposition initially to the grid northwest and then to the grid southwest, i.e. the plume was not stable in direction. Model predictions ranged from northwest to west, southwest and south, suggesting that the models could not fully reproduce the effect of an unstable plume direction. The predicted total activity deposited within the grid area ranged from 5.8 MBq to 3.4×10^6 MBq (measured, 2.3 MBq). The maximum predicted deposition ranged from 3.8×10^3 Bq m^{-2} to 5.6×10^9 Bq m^{-2} (measured, 1.9×10^4 Bq m^{-2}). Most of the model predictions showed the plume displaced significantly from the *y*-axis or going backwards (negative *y*-coordinate); the main apparent

---

[13] http://www.saga-gis.org/.

Figure 3. Wind speed (left) and wind direction (right) for the Kamenná field test conducted on 5 May 2009. The wind direction is shown with respect to both true north (left axis) and grid north (right axis). Data are 1 min averages. The triangles indicate the time of the detonation. The coordinates indicate the position (m) of the meteorological station with respect to the detonation point (0, 0). Measurements were taken at a height of 2 m.

Figure 4. Wind speed (left) and wind direction (right) for the Kamenná field test conducted on 14 July 2009. The wind direction is shown with respect to both true north (left axis) and grid north (right axis). Data are 1 min averages. The triangles indicate the time of the detonation. The coordinates indicate the position (m) of the meteorological station with respect to the detonation point (0, 0). Measurements were taken at a height of 2 m.

exception, HotSpot 2.07.01, does not actually account for plume direction. All predicted values of total activity deposited within the grid area exceeded the measured value, although several values (generated using CFD, CLMM and HotSpot 2.07.01 as used by Trifunović) were within a factor of four of the measured value. As in the earlier test, the assumptions about dry deposition velocity and source term partitioning appear to have been important in explaining differences in predictions.

4.3. Discussion

The EMRAS II exercises involved three main computational types of dispersion models. The Gaussian models used averaged meteorological data, while two of the Lagrangian models (University of Seville, LASAIR) used time-dependent meteorological data, corresponding to transient wind conditions. Appropriate handling of wind speed, and especially wind direction, is essential for obtaining good model predictions; in particular, use of averaged input data can cause errors in a simulation when there are rapid changes in wind direction.

The second exercise (14 July 2009) was more complicated than the first (5 May 2009) for at least two reasons. The second test had periods with no wind or very low wind speeds; these conditions are much more difficult to simulate, especially since models are generally validated for higher wind speeds. In addition, the two simulated small buildings in the grid area during the later test may have affected the plume behaviour by acting as obstacles to the wind flow. The wind measurements for these field tests were obtained at a height of
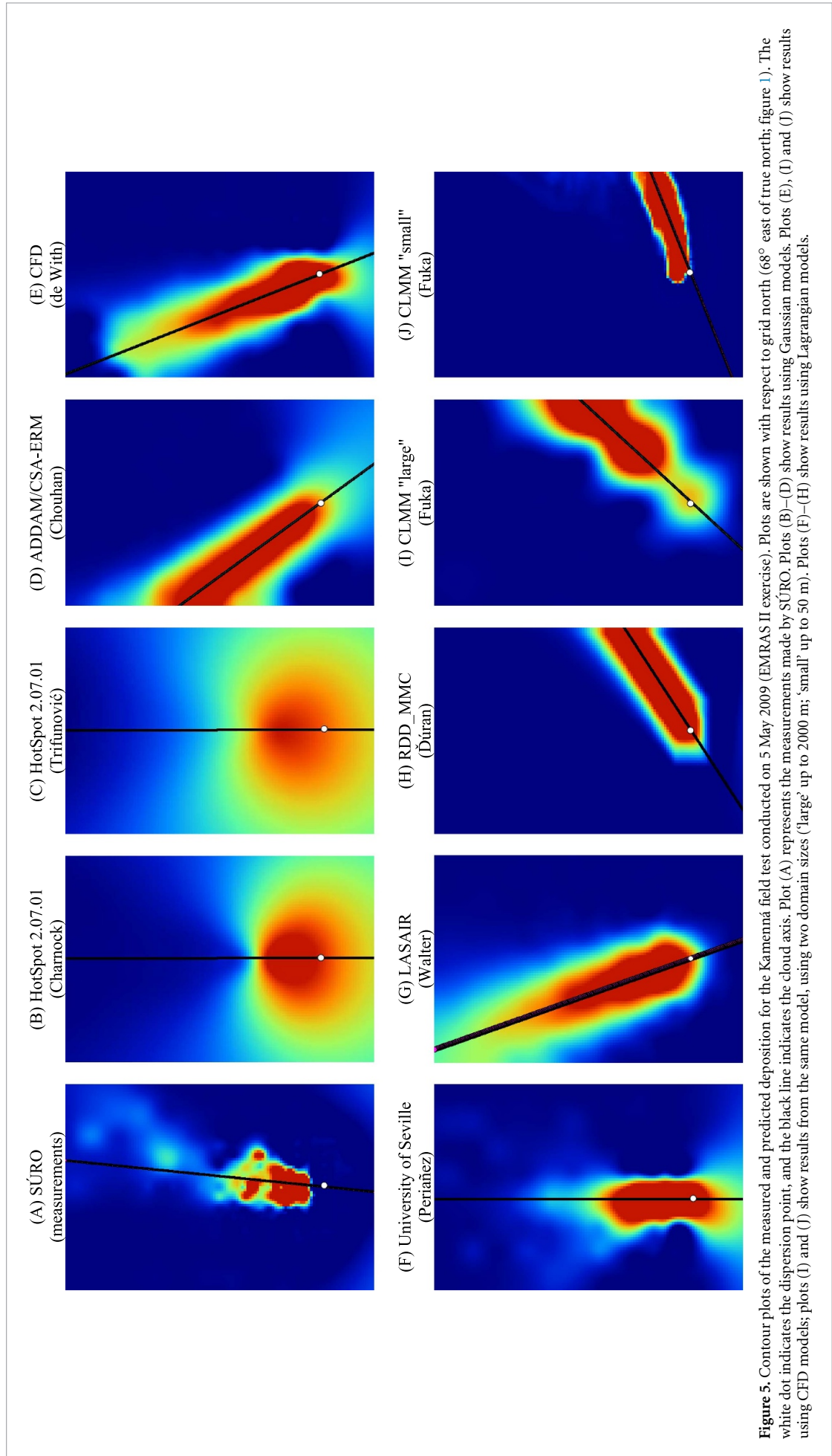
Figure 5. Contour plots of the measured and predicted deposition for the Kamenná field test conducted on 5 May 2009 (EMRAS II exercise). Plots are shown with respect to grid north (68° east of true north; figure 1). The white dot indicates the dispersion point, and the black line indicates the cloud axis. Plot (A) represents the measurements made by SÚRO. Plots (B)–(D) show results using Gaussian models. Plots (E), (I) and (J) show results using CFD models; plots (I) and (J) show results from the same model, using two domain sizes ('large' up to 2000 m; 'small' up to 50 m). Plots (F)–(H) show results using Lagrangian models.
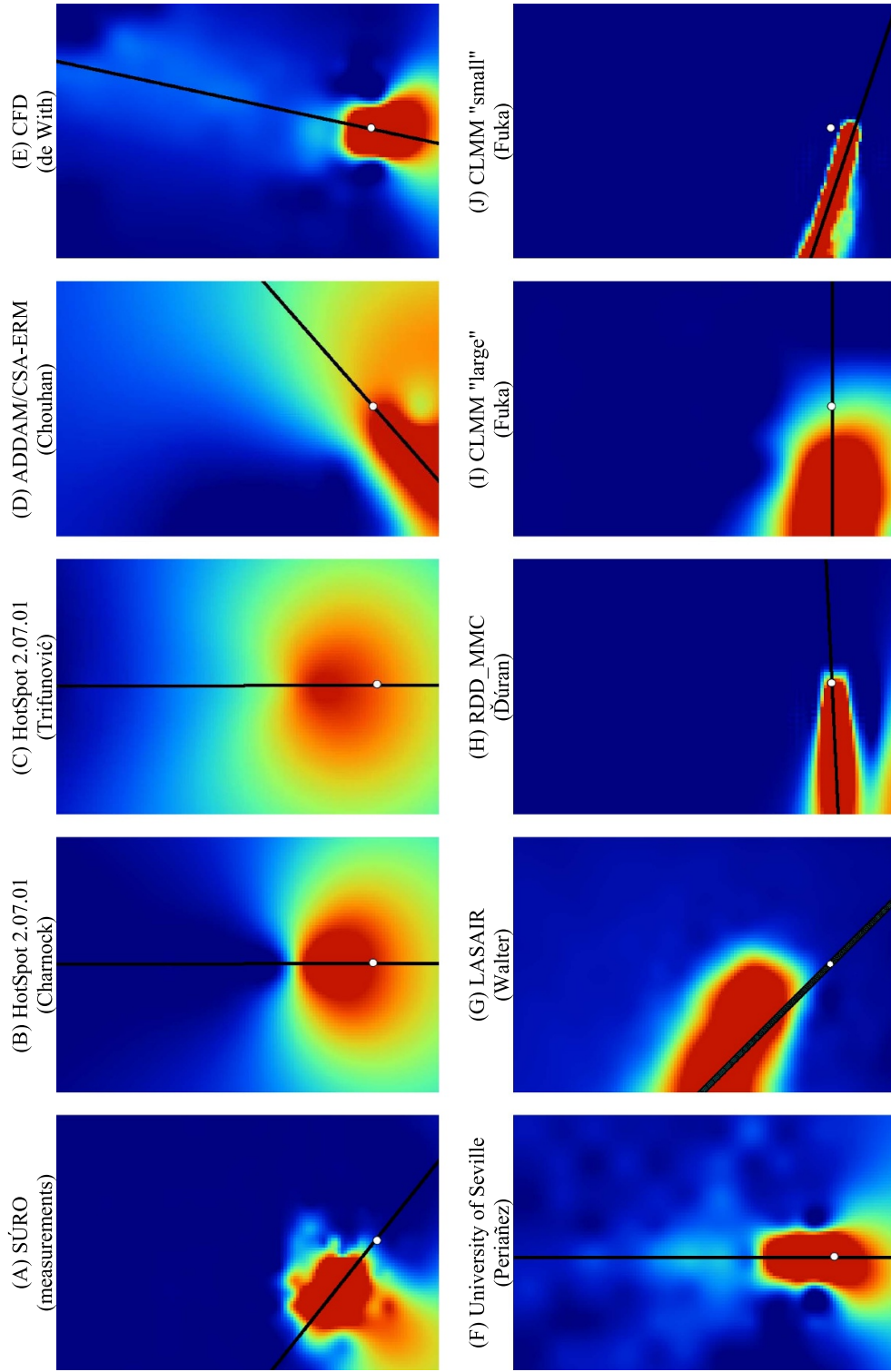
Figure 6. Contour plots of the measured and predicted deposition for the Kamenná field test conducted on 14 July 2009 (EMRAS II exercise). Plots are shown with respect to grid north ($68°$ east of true north; figure 1). The white dot indicates the dispersion point, and the black line indicates the cloud axis. Plot (A) represents the measurements made by SÚRO. Plots (B)–(D) show results using Gaussian models. Plots (E), (I) and (J) show results using CFD models; plots (I) and (J) show results from the same model, using two domain sizes ('large' up to 2000 m; 'small' up to 50 m). Plots (F)–(H) show results using Lagrangian models.

Table 7. Predicted and measured maximum values of deposited activity and total activity deposited within the grid area for the Kamenná field test conducted on 5 May 2009[a].

Model	Coordinates[b]		Maximum deposited activity (Bq m^{-2})	Total activity deposited within the grid area (MBq)
	x	y		
Measurements (SÚRO)	0	4.0	1.4×10^6	36
		Model predictions		
ADDAM/CSA-ERM (Chouhan)	−12.5	16.5	2.5×10^5	120
HotSpot 2.07.1 (Charnock)	0	8.0	1.0×10^6	730
HotSpot 2.07.1 (Trifunović)	0	8.0	1.3×10^3	1.8
RDD_MMC (Ďuran)	5.5	3.5	1.4×10^5	23
University of Seville (Periáñez)	−2.5	2.5	4.7×10^5	85
LASAIR (Walter)	−2.5	6.5	1.2×10^5	52
CFD (de With)	−1.0	5.0	1.1×10^4	3.1
CLMM—'large' (Fuka)	10.5	10.5	7.9×10^3	1.8
CLMM—'small' (Fuka)	1.0	2.5	4.9×10^4	1.9

[a] The total dispersed activity for the Kamenná field test conducted on 5 May 2009 was 1222 MBq of ^{99m}Tc.

[b] Coordinates for the locations of the maximum predicted and measured activities, assuming a dispersion point (origin of the explosion) at (0, 0); distances are in m.

Table 8. Predicted and measured maximum values of deposited activity and total activity deposited within the grid area for the Kamenná field test conducted on 14 July 2009[a].

Model	Coordinates[b]		Maximum deposited activity (Bq m^{-2})	Total activity deposited within the grid area (MBq)
	x	y		
Measurements (SÚRO)	−6.0	5.0	1.9×10^4	2.3
		Model predictions		
ADDAM/CSA-ERM (Chouhan)	−4.5	−3.5	6.4×10^5	360
HotSpot 2.07.1 (Charnock)	0	8.0	5.6×10^9	3.4×10^6
HotSpot 2.07.1 (Trifunović)	0	8.0	3.8×10^3	6.0
RDD_MMC (Ďuran)	−3.5	−0.5	1.2×10^6	83
University of Seville (Periáñez)	−2.5	2.5	5.7×10^5	94
LASAIR (Walter)	−6.0	12.5	2.4×10^5	79
CFD (de With)	0.0	−0.5	4.6×10^4	5.8
CLMM—'large' (Fuka)	−12.5	−1.0	3.4×10^4	8.6
CLMM—'small' (Fuka)	−3.0	−2.0	1.8×10^5	7.4

[a] The total dispersed activity for the Kamenná field test conducted on 14 July 2009 was 1088 MBq of ^{99m}Tc.

[b] Coordinates for the locations of the maximum predicted and measured activities, assuming a dispersion point (origin of the explosion) at (0, 0); distances are in m.

2 m, rather than the standard 10 m, and are more likely to have been influenced by the topography, including the simulated structures.

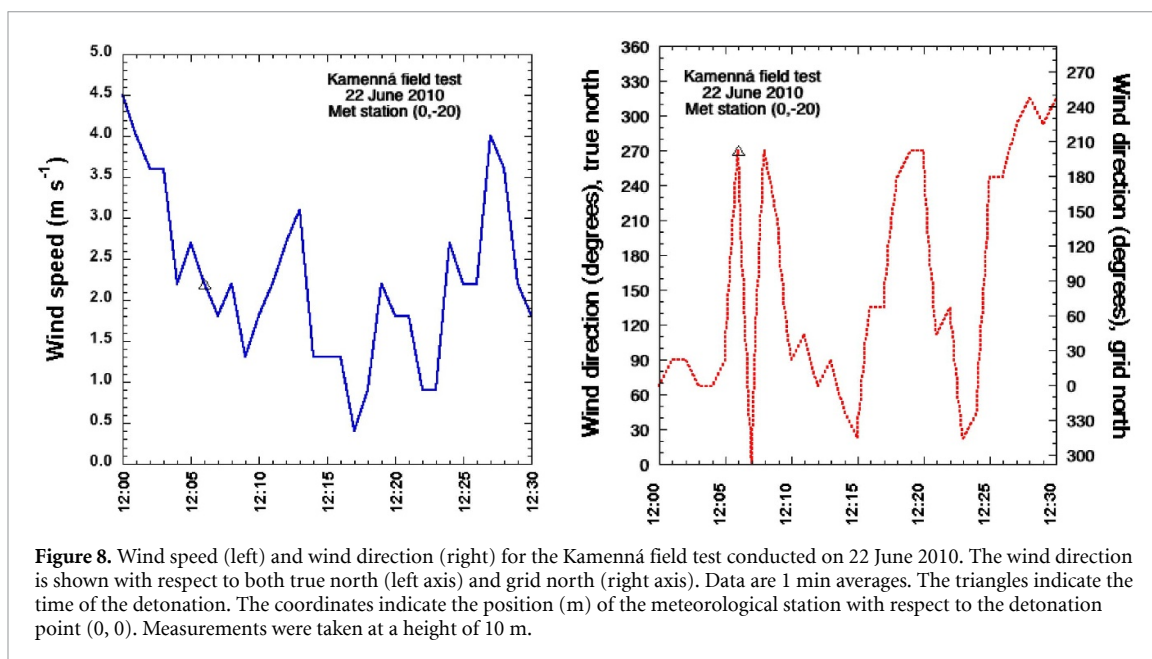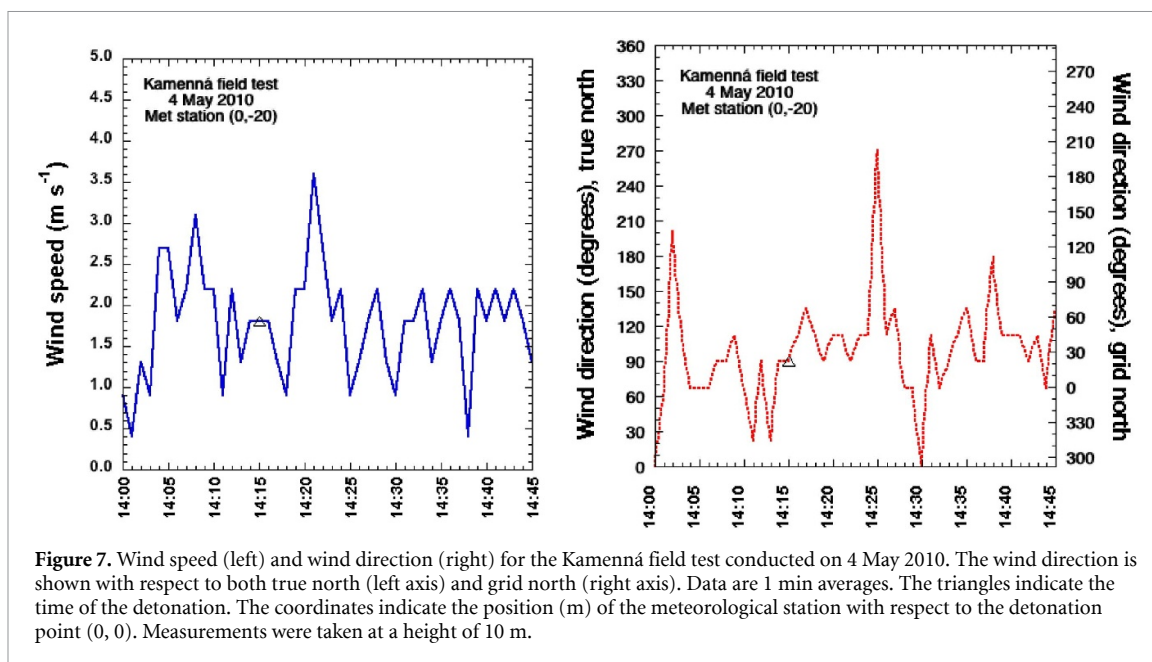## 5. MODARIA I exercises (Kamenná field tests 4 May 2010 and 22 June 2010)

5.1. Meteorological situation during the field tests

Figures 7 and 8 show the 1 min averaged wind speed and wind direction at a height of 10 m for the Kamenná field tests conducted on 4 May 2010 and 22 June 2010, respectively. The measuring equipment was located 20 m behind the dispersion point (grid coordinates (0, −20)). As seen in the figures, the meteorological conditions were not homogeneous for either of these field tests.

In the first of these tests (4 May 2010) the wind speed was 1.8 m s^{-1} at the time of the detonation, dropping below 1 m s^{-1} about 2 min later, increasing significantly to 3.6 m s^{-1} for about 2 min and then falling to an average of 1.5 m s^{-1}. The wind direction was steady at about 90° for about 8 min after the detonation, followed by two peaks (270° and 0°) then becoming steady at about 90° once again.

In the second test (22 June 2010), the wind speed fell from about 2.2 m s^{-1} at the time of the detonation to 1.4 m s^{-1}, and then varied between 0.4 and 3.1 m s^{-1} during the next 12 min. The wind direction varied even more widely, changing from 270° to 0° and back within the first 2 min, changing counterclockwise from 270° to 20° during the next 8 min, and then coming back to 270° for the next 4 min. This is typical of

Figure 7. Wind speed (left) and wind direction (right) for the Kamenná field test conducted on 4 May 2010. The wind direction is shown with respect to both true north (left axis) and grid north (right axis). Data are 1 min averages. The triangles indicate the time of the detonation. The coordinates indicate the position (m) of the meteorological station with respect to the detonation point (0, 0). Measurements were taken at a height of 10 m.

Figure 8. Wind speed (left) and wind direction (right) for the Kamenná field test conducted on 22 June 2010. The wind direction is shown with respect to both true north (left axis) and grid north (right axis). Data are 1 min averages. The triangles indicate the time of the detonation. The coordinates indicate the position (m) of the meteorological station with respect to the detonation point (0, 0). Measurements were taken at a height of 10 m.

an unstable convective situation in which air masses are lifted (e.g. due to insolation), thereby changing the main wind direction; once the updraft has finished, the main wind direction again prevails.

5.2. Results

Figures 9 and 10 provide comparisons of the measured and predicted activity concentrations (deposition, Bq m^{-2}) for the two field tests. Tables 9 and 10 summarize the maximum measured and predicted deposition (Bq m^{-2}) for each of the respective field tests, and the total measured and predicted activity deposited in the grid area (MBq) for each field test.

For the first test (4 May 2010), the measurements indicated deposition largely to the grid east, with an early component to the north and a later component to the south (figure 9). In contrast, the models predicted the primary deposition to west-northwest, south-southwest and southeast (the last looks like dispersion to the south-southwest, but displaced to the east of the dispersion point.). The predicted total activity deposited within the grid area ranged from 67 MBq to 334 MBq (measured, 202 MBq). The predicted maximum deposition ranged from 5.9×10^5 Bq m^{-2} to 1.4×10^6 Bq m^{-2} (measured, 2.1×10^6 Bq m^{-2}). For the total activity deposited within the grid, one prediction (URD, developed by the DTU) was very close to the measured value, while the other two predictions were about a factor of 3 lower

Table 9. Predicted and measured maximum values of deposited activity and total activity deposited within the grid area for the Kamenná field test conducted on 4 May 2010[a].

| Model | Coordinates[b] | | Maximum deposited activity (Bq m^{-2}) | Total activity deposited within the grid area (MBq) |
	x	y		
Measurements (SÚRO)	0	3.0	2.1×10^6	202
Model predictions				
ADDAM/CSA-ERM (Chouhan)	−5.0	1.0	6.3×10^5	334
URD (Tay)	6.0	−9.0	1.4×10^6	207
LASAIR (Walter)	−1.0	−6.0	5.9×10^5	67.2

[a] The total dispersed activity for the Kamenná field test conducted on 4 May 2010 was 2119 MBq of ^{99m}Tc.

[b] Coordinates for the locations of the maximum predicted and measured activities, assuming a dispersion point (origin of the explosion) at (0, 0); distances are in m.

Table 10. Predicted and measured maximum values of deposited activity and total activity deposited within the grid area for the Kamenná field test conducted on 22 June 2010[a].

| Model | Coordinates[b] | | Maximum deposited activity (Bq m^{-2}) | Total activity deposited within the grid area (MBq) |
	x	y		
Measurements (SÚRO)	0	3.0	9.6×10^5	38.0
Model predictions				
ADDAM/CSA-ERM (Chouhan)	0.5	4.5	5.3×10^5	382
URD (Tay)	5.5	−8.5	6.4×10^5	123
LASAIR (Walter)	3.0	5.5	5.3×10^5	189

[a] The total dispersed activity for the Kamenná field test conducted on 22 June 2010 was 2045 MBq of ^{99m}Tc.

[b] Coordinates for the locations of the maximum predicted and measured activities, assuming a dispersion point (origin of the explosion) at (0, 0); distances are in m.
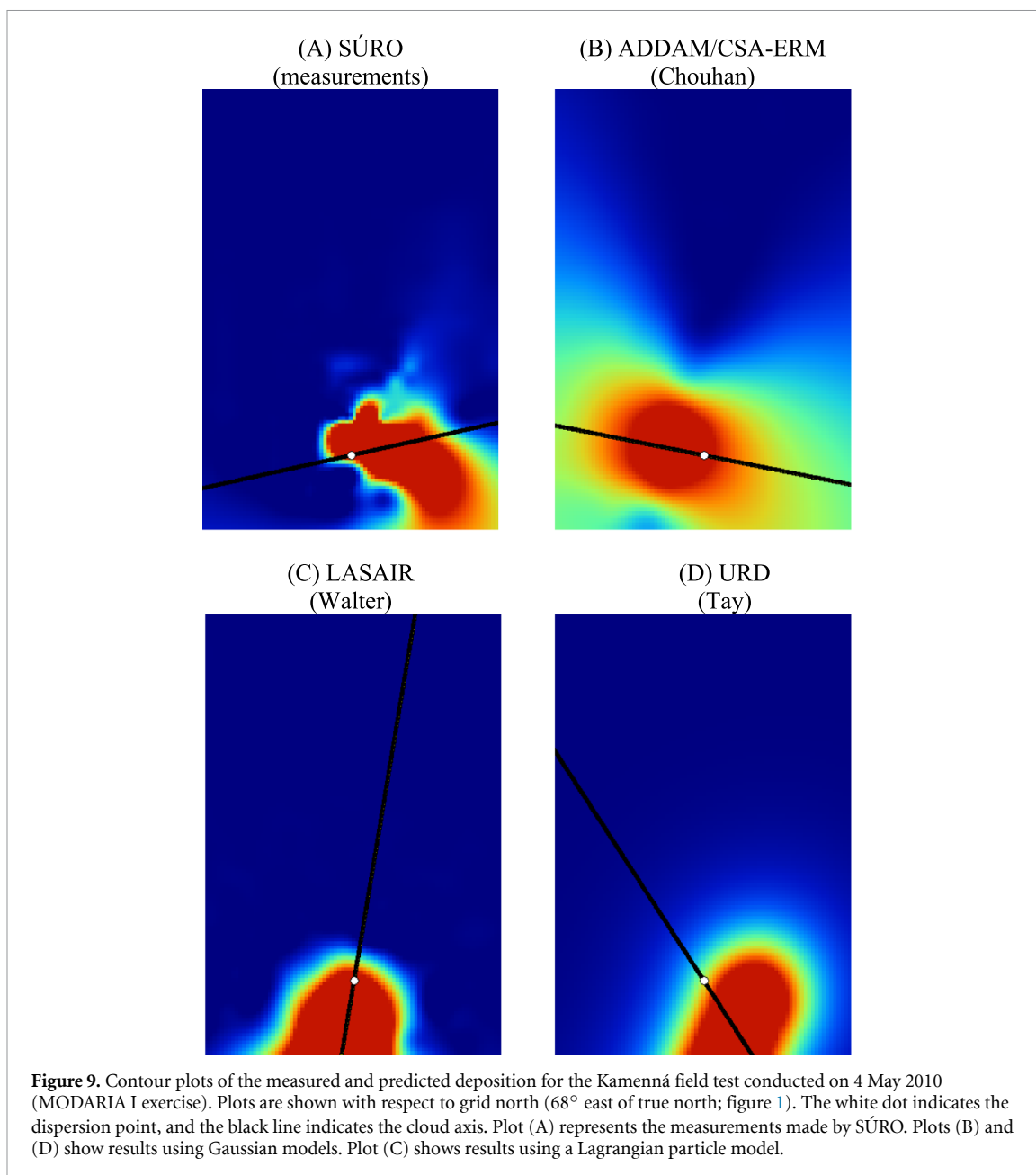
(LASAIR) or 1.6 higher (ADDAM/CSA-ERM). For the maximum deposited activity, model predictions ranged from about 30% to 70% of the measured value.

For the second test (22 June 2010), two models (ADDAM/CSA-ERM and LASAIR) predicted the general direction of the highest-concentration portion of the plume reasonably well (figure 10), in spite of the large fluctuations in wind direction. The third model (URD) also predicted the general direction of the plume, although the predicted location of highest concentration differed from the measurements. The predicted total activity deposited within the grid area ranged from 123 MBq to 382 MBq (measured, 38 MBq). The predicted maximum deposition ranged from 5.3×10^5 Bq m^{-2} to 6.4×10^5 Bq m^{-2} (measured, 9.6×10^5 Bq m^{-2}). For the total activity deposited within the grid, the predictions ranged from 3 to 10 times higher than the measured value. For the maximum deposited activity, model predictions ranged from about 55% to 70% of the measured value. Although the predicted maximum values for deposited activity were less than the measured maximum value, the predicted values for total activity deposited within the grid area were larger than the measured value, probably due to larger areas predicted to be affected by the plume than, in fact, was the case.

5.3. Discussion

For both field tests, the measurements indicated that the plume was not stable in direction during the deposition event. For the first test (4 May 2010), the models did not reproduce the effect of the unstable plume (figure 9). For the second test (22 June 2010), two models (ADDAM/CSA-ERM and LASAIR) predicted the highest concentration portion of the plume reasonably well (figure 10), in spite of the large fluctuations in wind direction.

The three models used in these exercises (ADDAM/CSA-ERM, LASAIR and URD) differed in computational type (Gaussian or Lagrangian), handling of meteorological data (use of averaged or time-dependent data), dry deposition velocity, atmospheric stability class and other assumptions (tables 3 and 5). These differences are likely to explain the differences in the model predictions. For example, the ADDAM/CSA-ERM model gave the highest values for predicted deposition in the exercises (tables 9 and 10), consistent with its use of the highest value for dry deposition velocity (table 5). More details on the possible reasons for differences between models are provided in the Working Group 2 report (IAEA 2021).

Figure 9. Contour plots of the measured and predicted deposition for the Kamenná field test conducted on 4 May 2010 (MODARIA I exercise). Plots are shown with respect to grid north (68° east of true north; figure 1). The white dot indicates the dispersion point, and the black line indicates the cloud axis. Plot (A) represents the measurements made by SÚRO. Plots (B) and (D) show results using Gaussian models. Plot (C) shows results using a Lagrangian particle model.

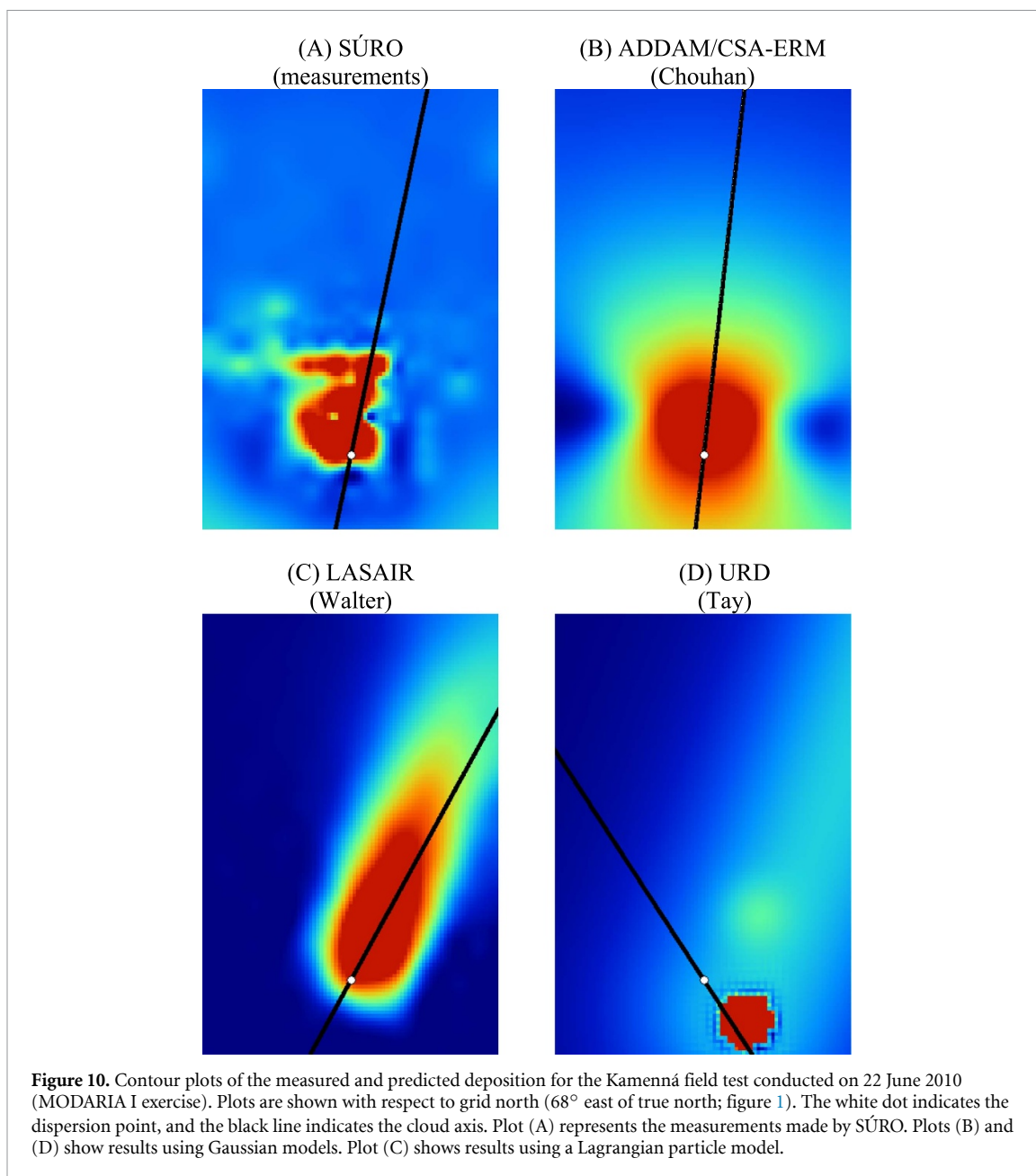## 6. MODARIA II exercise (Boletice field test 17 June 2014)

6.1. Meteorological situation during the field test

Figure 11 shows the wind speed and direction at heights of 2 m and 10 m and at 1 s intervals. The time in minutes is relative to the detonation time ($t = 0$). The meteorological station was located 110 m northeast of the dispersion point. The wind speed immediately after the detonation varied from about 2 km h^{-1} to 8 km h^{-1} at a height of 2 m and from about 7 km h^{-1} down to 1 km h^{-1} at a height of 10 m. The wind direction appears to have shifted from about 240° at the time of the detonation to about 270°–300° (2 m) or 300°–330° (10 m) a few minutes after the detonation.

6.2. Results

Figure 12 provides a comparison of the measured and predicted activity concentrations (deposition, Bq m^{-2}) for the field test. The measurements and predictions were normalized to the maximum measured or predicted deposition (1 = the maximum measured or predicted deposition, as relevant). Table 11 summarizes the maximum measured and predicted deposition (Bq m^{-2}) for the field test and the total measured and predicted activity deposited in the grid area (MBq) for the field test.

The measurements indicated deposition largely to the grid southeast (figure 12). Both sets of predictions using LASAIR showed a similar direction of the plume, as did the HotSpot 3.1 prediction by Mancini and the second HotSpot 3.0.3 prediction by Charnock. The first prediction by Charnock showed the plume going to

Figure 10. Contour plots of the measured and predicted deposition for the Kamenná field test conducted on 22 June 2010 (MODARIA I exercise). Plots are shown with respect to grid north (68° east of true north; figure 1). The white dot indicates the dispersion point, and the black line indicates the cloud axis. Plot (A) represents the measurements made by SÚRO. Plots (B) and (D) show results using Gaussian models. Plot (C) shows results using a Lagrangian particle model.

the northeast; the second prediction included an adjustment to the timing of the meteorological data to allow for the distance (110 m) between the meteorological station and the dispersion point, resulting in the predicted plume going to the southeast, similar to the other model predictions. As shown in table 6, the two sets of HotSpot 3.0.3 predictions by Charnock varied only in the wind speed and direction used for the calculations. Walter adjusted the timing of the meteorological data by 2 min to allow for the distance between the meteorological station and the dispersion point. Mancini, based on observations from the videos of the event, adjusted the reported wind directions by 45° to account for differences between the meteorological station and the dispersion point.

The total activity deposited within the grid area, as predicted by two users of LASAIR, ranged from 73.8 MBq to 200 MBq (measured, 41.3 MBq), exceeding the measured value by factors of 1.8 (Walter) and 4.8 (Mancini). Total deposited activity was not calculated for the HotSpot predictions, since the predictions did not include all of the grid area.

The predicted maximum deposition ranged from 9.0×10^3 Bq m^{-2} to 5.4×10^6 Bq m^{-2} (measured, 8.6×10^5 Bq m^{-2}). Model predictions for the maximum deposited activity ranged from about 1% of the measured value to about a factor of 6 greater than the measured value. All of the model predictions put the maximum deposited activity at a greater distance from the dispersion point than the actual measured maximum deposition.
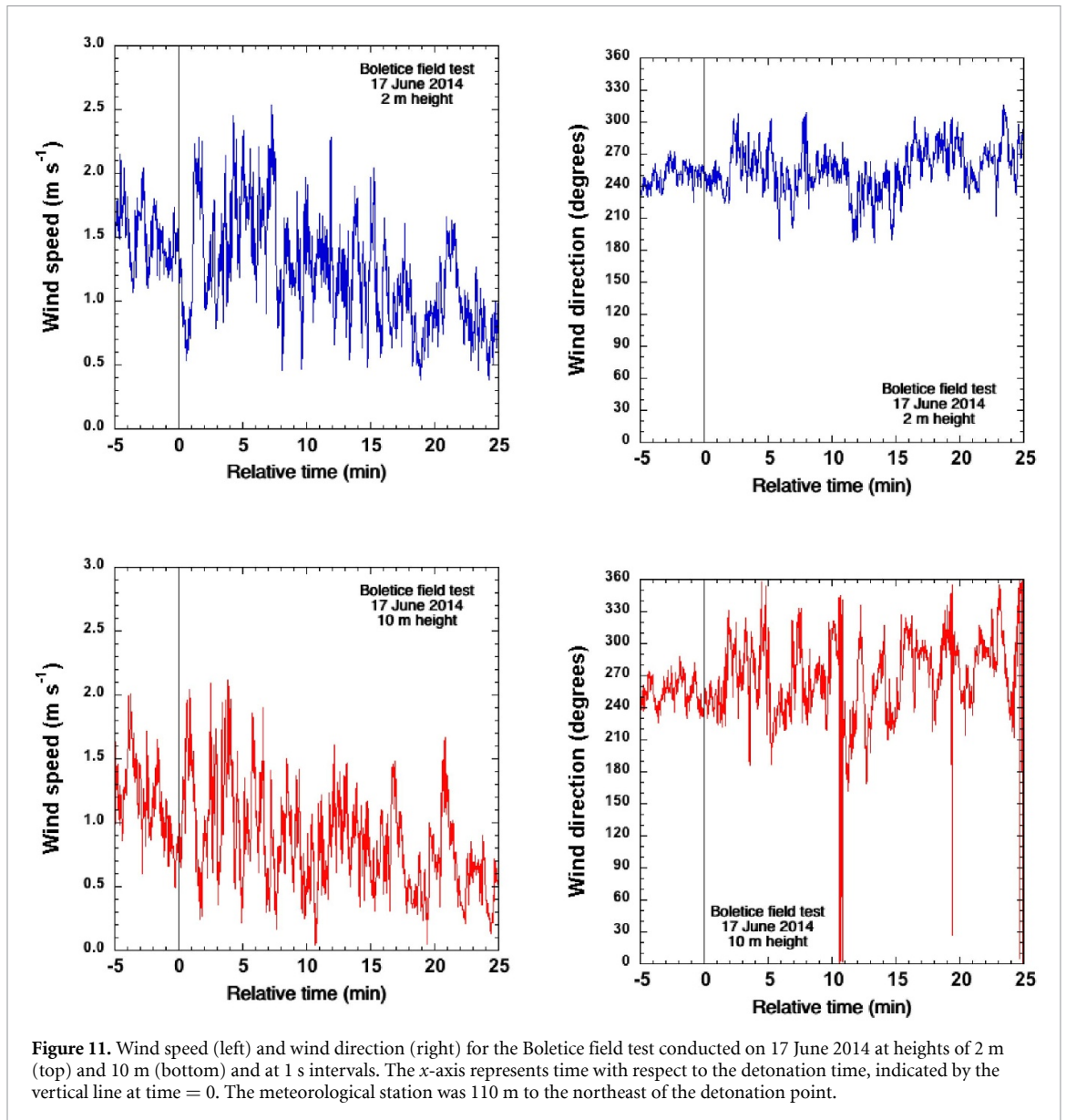
Figure 11. Wind speed (left) and wind direction (right) for the Boletice field test conducted on 17 June 2014 at heights of 2 m (top) and 10 m (bottom) and at 1 s intervals. The *x*-axis represents time with respect to the detonation time, indicated by the vertical line at time = 0. The meteorological station was 110 m to the northeast of the detonation point.

6.3. Discussion

The Boletice exercise provided the opportunity to compare model predictions with measurements for a different context than the previous field tests (EMRAS II and MODARIA I exercises, described above). The results of the exercise included predictions from two participants using the same model (Walter and Mancini using LASAIR), two participants using different versions of the same model (Charnock using HotSpot 3.0.3 and Mancini using HotSpot 3.1) and one participant using two models (Mancini using HotSpot 3.1 and LASAIR). For HotSpot 3.0.3 and 3.1, Charnock and Mancini differed in their choice of atmospheric stability class, particle size distribution and height of the cloud top (table 6). Charnock's second prediction used wind speed and direction similar to those used by Mancini. For LASAIR, Walter and Mancini differed in their choice of atmospheric stability class, range of wind directions, and particle size distribution.

For both the HotSpot 3.1 and LASAIR models, Mancini manually shifted the wind directions by 45° to match the observations from the videos of the detonation. Walter and Charnock also modified the wind data, Walter by adjusting the timing of the meteorological data by 2 min and Charnock by selecting average values for wind speed and direction, with the latter being consistent with the observed direction of the plume. In the previous exercises, the meteorological station was located 20 m or less from the dispersion point; in this exercise it was 110 m from the dispersion point. All three participants adjusted for this distance, either by delaying time-dependent data (Walter, Charnock) or adjusting the angle to match observations from videos (Mancini), and all with reasonable success. This finding suggests the importance of having meteorological data as close as possible to the dispersion point, or adjusted for the distance between them. It also suggests
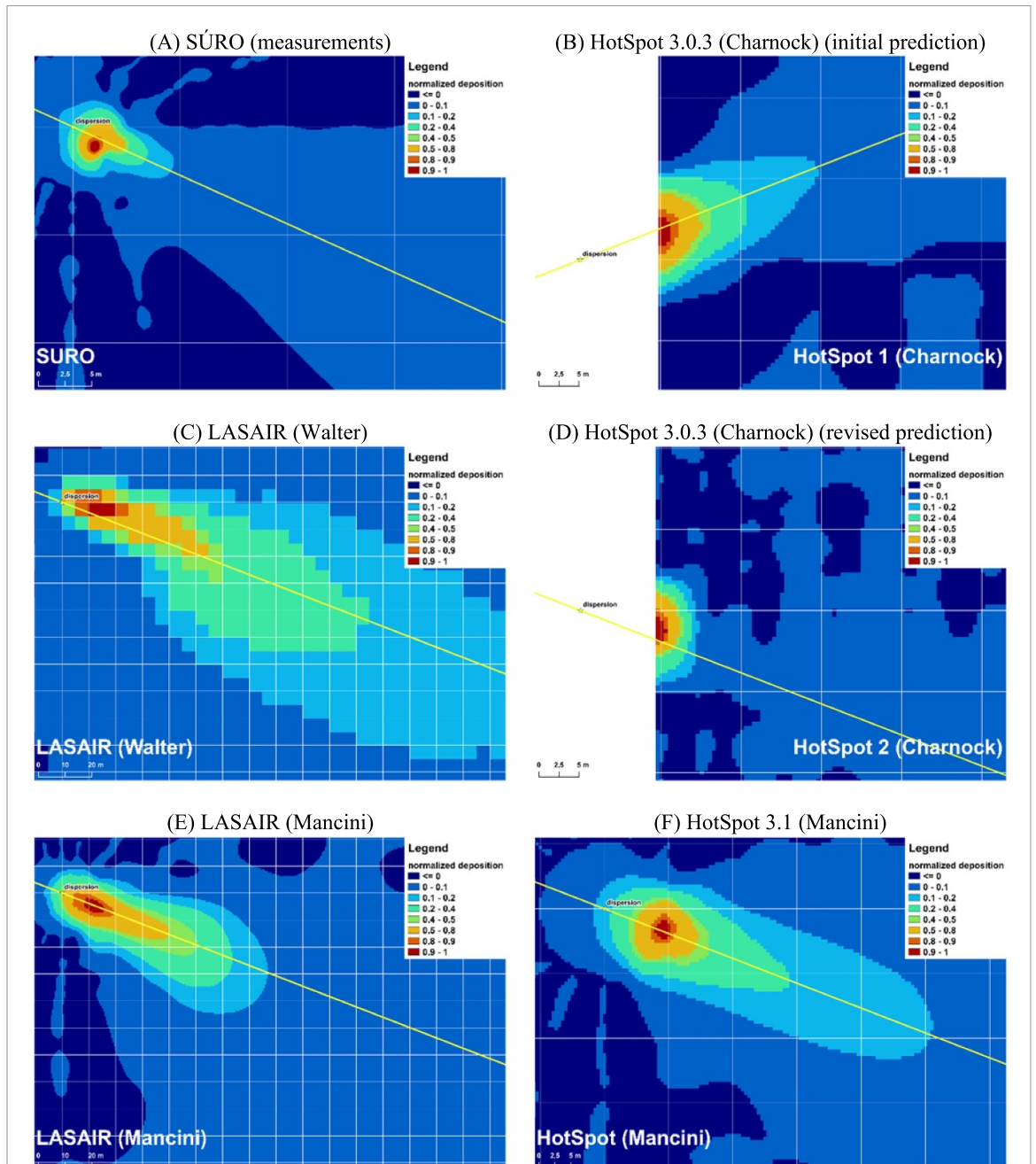
Figure 12. Contour plots of the measured and predicted deposition for the Boletice field test conducted on 17 June 2014 (MODARIA II exercise). Data are normalized to the maximum measured or predicted deposition (1 = the maximum measured or predicted deposition). The star indicates the dispersion point, and the line indicates the cloud axis. Plot (A) represents the measurements made by SÚRO. Plots (B), (D) and (F) show results using two versions of HotSpot, which is a Gaussian model. Plots (C) and (E) show results using LASAIR, which is a Lagrangian model. The two plots for HotSpot as used by Charnock show the predictions before and after an adjustment of the meteorology (see text). The predictions by Charnock did not include the first 10 m of the grid area. Note that the plots are on different scales.

that modelling this type of event could be more difficult without an onsite meteorological station, for example, in the case of an unplanned dispersion event when only regional meteorological data are available.

Comparison of the predicted maximum deposited activities shows similar predicted locations for both users of HotSpot (Charnock's second predictions, compared with Mancini), and for both users of LASAIR (Walter and Mancini), although the magnitudes of the predicted maximum deposited activities varied (for HotSpot, by a factor of 15 between Charnock's second prediction and Mancini's prediction; for LASAIR, by a factor of about 5 between Mancini and Walter). Mancini's predictions using two models differed from each other by a factor of about 3, consistent with the same input assumptions being used for both models.

Table 11. Predicted and measured maximum values of deposited activity and total activity deposited within the grid area for the Boletice field test of 17 June 2014[a].

Model	Coordinates[b] x	Coordinates[b] y	Maximum deposited activity (Bq m^{-2})	Total activity deposited within the grid area (MBq)
Measurements (SÚRO)	2	−1.9	8.6×10^5	41.3
Model predictions				
HotSpot 3.0.3 (1) (Charnock)	10	3.5	9.0×10^3	—[c]
HotSpot 3.0.3 (2) (Charnock)	9.6	−2.5	5.4×10^6	—[c]
HotSpot 3.1 (Mancini)	9	−3	3.6×10^5	—[c]
LASAIR (Walter)	12.29	−2.72	2.3×10^4	73.8
LASAIR (Mancini)	12.5	−5	1.1×10^5	200

[a] The total dispersed activity for the Boletice field test of 17 June 2014 was 713 MBq of ^{140}La.

[b] Coordinates for the locations of the maximum predicted and measured activities, assuming a dispersion point (origin of the explosion) at (0, 0); distances are in m.

[c] Not calculated. Some parts of the grid area were not included in the HotSpot predictions.

7. General findings from the exercises

The field tests described in this paper presented several challenges to participants in the modelling exercises. The exercises involved prediction of spatially varying deposition (surface activity concentration) using time-dependent wind conditions. The detonations themselves were not modelled directly in any of the exercises; participants started with the initial cloud or plume. In some exercises, participants were provided with a suggested set of default cloud dimensions and partitioning of the source term within the cloud, but often the characterizations of the initial cloud differed between modellers.

Model results varied, sometimes considerably, in the predicted directions of plumes for a given test, as seen in the contour plots (figures 5, 6, 9, 10 and 12). Predicted amounts of deposited activity also varied widely in some cases, although for any given exercise some of the predictions were reasonably close to the measurements. A number of factors potentially contribute to differences in model predictions, as follows:

- Three different computational approaches were used in these exercises, including Gaussian models, Lagrangian models and CFD models. The Gaussian approach has been applied successfully in many applications, but it is best suited for long-term releases and dispersion rather than the short-term release and dispersion considered in these exercises. CFD models can produce the highest accuracy for a simulation of dispersion following an instantaneous release, but they require considerable computing time. Lagrangian particle models typically do better than Gaussian models for short-term releases and dispersion, and typically offer the best balance between effort and accuracy, especially for emergency-response use.
- Some models were intended for grid or domain sizes larger or smaller than those used in the experiments.
- Values for dry deposition velocity, atmospheric stability class, dimensions of the initial cloud, particle size distribution and distribution of the activity within the initial cloud varied between participants, but were intended to be as close as possible to the real situation, depending on the particular model's capabilities. Detailed evaluation of parameter sensitivity for the various models is beyond the scope of these modelling exercises.
- Use of average versus time-dependent wind speeds and directions varied between models. In addition, selections of values for wind speed and direction varied between participants.

Uncertainty in model predictions may be due to uncertainty in input data or to model uncertainty; model uncertainty includes both the computational approach (model numerics) and model parameters. Different approaches may be used to evaluate key parameters for important processes (e.g. diffusion coefficients for turbulence), and different approaches may therefore lead to different model results. Some parameters may require site-specific information or calibration, which may not always be possible. Numerical solutions require temporal or spatial discretization (or both), and generally provide approximations to the real solution. In these exercises, models with different complexities and parameters were used to calculate radionuclide deposition on the ground, and differences in the model predictions are reasonably expected. While it is often assumed that if two models give similar results for some particular application, the simpler model is better than the complex model, Monte *et al* (2006) have pointed out that this assumption should be avoided. A simple model might not be sufficiently developed for application to the range of possible cases and circumstances that more complex and general models (i.e. more flexible models) are able to simulate.

For the Boletice exercise, participants compensated one way or another for the distance between the meteorological station and the dispersion point. This might not have mattered for the Kamenná exercises, for which the meteorological stations were much closer to the dispersion point (20 m or less), but it could be very important for other dispersion events, particularly unplanned events with only regional meteorological data available. These exercises involved a very small modelling domain, with the wind and turbulence assumed to be uniform in the horizontal plane; for larger domains, more detailed consideration of the wind and turbulence fields would be appropriate.

This set of field tests, at both the Boletice and Kamenná sites, demonstrated the need for the proper application of models in the context of existing physical effects (e.g. the detonations); in such cases, the models must be able to handle microscale conditions. In addition, these exercises were a first approach to simulate dispersion after an explosion for civilian experiments, and the results have been useful to improve the layout of such experiments, for example positioning of the meteorological stations.

Visual comparison of contour plots of measured and predicted deposition, using the same coordinate system and colour scale, provided a useful method for overall comparison of measurements and model predictions for a given field test. In some cases, the contour plot of the measurements indicated that the plume was not stable in direction during the deposition event; models generally were not able to fully reproduce the effect of an unstable plume direction.

Comparison of modelling results among participants and with the measurements provided an invaluable opportunity to discuss and explain differences in modelling approaches and the influence of the selection of parameter values on model predictions, with an opportunity to improve the models and how they are applied. These relatively simple models are able to give reasonably realistic results, quickly, and without requiring large numbers of input data that may be difficult or impossible to obtain.

Acknowledgments

ORCID iD

Kathleen M Thiessen ⬤ https://orcid.org/0000-0002-5564-7499

References

Homann S G 2009 HotSpot health physics codes version 2.07 user's guide *Lawrence Livermore National Laboratory* LLNL-TM-411345

IAEA 1994 Modelling the deposition of airborne radionuclides into the urban environment *First report of the VAMP Urban Working Group IAEA-TECDOC-760*

IAEA 2012a Environmental modelling for radiation safety (EMRAS) *A Summary Report of the Results of the EMRAS Programme (2003–2007) IAEA-TECDOC-1678*

IAEA 2012b Environmental modelling of remediation of urban contaminated areas *Report of the Urban Remediation Working Group of the EMRAS (Environmental Modelling for Radiation Safety) Programme. IAEA 2012a Environmental Modelling for Radiation Safety (EMRAS). A Summary Report of the Results of the EMRAS Programme (2003–2007) IAEA-TECDOC-1678*

IAEA 2021 Assessment of radioactive contamination in urban areas *Report of Working Group 9 Urban Areas of EMRAS II Topical Heading Approaches for Assessing Emergency Situations Environmental Modelling for Radiation Safety (EMRAS II) Programme IAEA-TECDOC-1941*

IAEA 2022 Assessment of radioactive contamination and effectiveness of remedial measures in urban environments *Report of Working Group 2 of the MODARIA (Modelling and Data for Radiological Impact Assessments) Programme* (in preparation)

IAEA Assessment of radioactive contamination, exposures, and countermeasures in urban environments *Report of Working Group 2 of the MODARIA II (Modelling and Data for Radiological Impact Assessments) Programme* (in preparation)

Lee S, Wolberg G and Shin S Y 1997 Scattered data interpolation with multilevel B-splines *IEEE Trans. Vis. Comput. Graph.* **3** 228–44

Monte L, Håkanson L, Periáñez R, Laptev G, Zheleznyak M, Maderich V, Angeli G and Koshebutsky V 2006 Experiences from a case study of multi-model application to assess the behaviour of pollutants in the Dnieper-Bug estuary *Ecol. Modell.* **195** 247–63

Prouza Z, Beckova V, Cespirova I, Helebrant J, Hulka J, Kuca P, Michalek V, Rulik P, Skrkal J and Hovorka J 2010 Field tests using radioactive matter *Radiat. Prot. Dosim.* **139** 519–31

Thiessen K M *et al* 2008 Improvement of modelling capabilities for assessing urban contamination: the EMRAS Urban Remediation Working Group *Appl. Radiat. Isot.* **66** 1741–4

Thiessen K M *et al* 2011 Assessing emergency situations and their aftermath in urban areas: the EMRAS II Urban Areas Working Group *Radioprotection* **46** S601–7

Thiessen K M *et al* 2022 Urban working groups in the IAEA's model testing programmes: overview from the MODARIA I and MODARIA II programmes *J. Radiat. Protect.* **42** 020502

Urso L, Kaiser J C, Woda C, Helebrant J, Hulka J, Kuca P and Prouza Z 2014 A fast and simple approach for the estimation of a radiological source from localised measurements after the explosion of a radiological dispersal device *Radiat. Prot. Dosim.* **158** 453–60